



Contents lists available at SciVerse ScienceDirect

Spectrochimica Acta Part A: Molecular and Biomolecular Spectroscopy

journal homepage: www.elsevier.com/locate/saa

Synthesis, X-ray crystal structure and optical properties of novel 1,3,5-triarylpyrazoline derivatives and the fluorescent sensor for Cu²⁺

Sheng-Qing Wang, Ying Gao, Hao-Yan Wang, Xiao-Xin Zheng, Shi-Li Shen, Yan-Ru Zhang, Bao-Xiang Zhao*

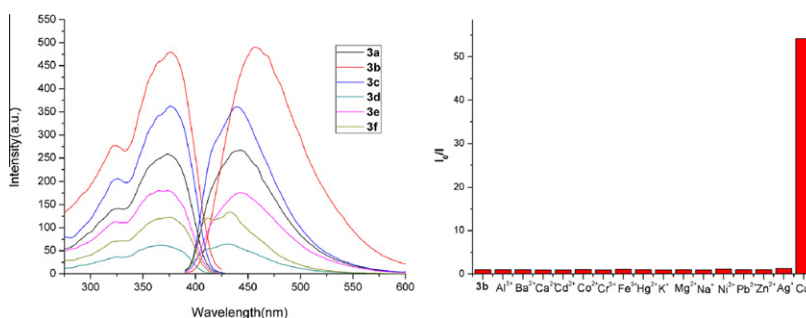
Institute of Organic Chemistry, School of Chemistry and Chemical Engineering, Shandong University, Jinan 250100, PR China

HIGHLIGHTS

- ▶ A series of 1,3,5-triarylpyrazoline derivatives were synthesized.
- ▶ These derivatives exhibited large Stokes shifts.
- ▶ The compound **3b** can be used to determine Cu²⁺ ion.
- ▶ The sensor is very sensitive with fluorometric detection limit of 2.46×10^{-8} M.

GRAPHICAL ABSTRACT

A series of 1,3,5-triarylpyrazoline derivatives were synthesized. These derivatives exhibited large Stokes shifts. The compound **3b** can be used to determine Cu²⁺ ion. The sensor is very sensitive with fluorometric detection limit of 2.46×10^{-8} M.



ARTICLE INFO

Article history:

Received 12 October 2012
 Received in revised form 29 November 2012
 Accepted 13 December 2012
 Available online 10 January 2013

Keywords:

Pyrazoline
 Synthesis
 X-ray
 UV absorption
 Fluorescent sensor
 Copper ion

ABSTRACT

A series of novel 1,3,5-triarylpyrazoline derivatives was synthesized by the reaction of chalcone and 5-aryl-2-hydrazinyl-1,3,4-thiadiazole in 43.3–84.7% yields. The structures of compounds were characterized using IR, ¹H NMR and HRMS spectroscopy and X-ray diffraction analysis. The absorption and fluorescence characteristics of the compounds were investigated in dichloromethane, toluene, acetonitrile, *N,N*-dimethylformamide and tetrahydrofuran. The results showed that the absorption maxima of the compounds vary from 366 to 370 nm depending on the group bound to benzene rings. The maximum emission spectra of the compounds in dichloromethane were dependent on nature of groups in benzene ring. Furthermore, the compound **3b** can be used to determine Cu²⁺ ion with high selectivity and a low detection limit in the DMF:H₂O = 1:1 (v/v) solution.

© 2012 Elsevier B.V. All rights reserved.

Introduction

Pyrazolines are important nitrogen-containing 5-membered heterocyclic compounds with a wide range of interesting properties, such as antimicrobial [1], antiameobic [2], anticancer [3], anti-

depressant [4], antihepatotoxic [5], antitubercular [6], antimalarial [7] and anti-inflammatory [8]. Furthermore, pyrazoline derivatives show stronger fluorescence, and have higher hole-transport efficiency and excellent emitting blueness property. Therefore, pyrazoline derivatives have widely been used as whitening or brightening reagents for synthetic fibers, fluorescent chemosensors for recognition of transition metal ions, hole-transport materials in the electrophotography and electroluminescence fields [9–17].

* Corresponding author. Tel.: +86 531 88366425; fax: +86 531 88564464.
 E-mail address: bxzhao@sdu.edu.cn (B.-X. Zhao).

Meanwhile, pyrazolone-5 derivatives which are similar to pyrazoline form an important class of organic compounds due to their coordination behaviour with metals [18,19] and biological activity [20]. Considerable attempts have been made to synthesize and elucidate the effects of substituent on the absorption and fluorescence properties of pyrazolines with structure diversity [21–26]. Moreover, pyrazoline with membrane permeability, low toxicity, and high quantum yield render the fluorophore attractive for biological applications [27,28]. Recently, a pyrazoline as effective “turn on” fluorescent sensors in acetonitrile for Cd^{2+} and Zn^{2+} was also reported [29].

The production of fluorescent devices for the sensing and reporting of chemical events is currently of significant importance for both chemistry and biology [30]. Among them, sensing of Cu^{2+} has received ever-increasing attention, since Cu^{2+} plays a crucial role as a catalytic co-factor for a variety of metalloenzymes, including superoxide dismutase, cytochrome *c* oxidase, tyrosinase and so on [31]. However, under overloading conditions, Cu^{2+} can cause oxidative stress and disorders associated with neurodegenerative diseases, such as Alzheimer's disease, Wilson's disease, and Menke's disease, probably by its involvement in the production of reactive oxygen species [32]. Therefore, selective and rapid detection of Cu^{2+} in physiological samples is of toxicological and environmental concern [33–35].

It is known that the aryl substituents in the 1- and 3-position of the pyrazoline ring influence the photophysical properties of the fluorophores in distinctly different ways [28,36,37]. Thus, one might expect to modify the pyrazoline structure by changes of the substituent in the 1- and 3-position. As an extension of our work on the development of fluorescent probe for monitoring metal ions [9,10,38–40], in this paper, we synthesized a series of novel pyrazoline compounds containing 1,3,4-thiadiazole groups in 1-position using 5-aryl-2-hydrazinyl-1,3,4-thiadiazole and chalcones (Scheme 1), which had good blue light fluorescence. These compounds have not been reported previously. The compounds were characterized by IR, ^1H NMR, HRMS, X-ray diffraction analysis and fluorescence techniques. It is found that ICT (intramolecular charge transfer) process exists between the nitrogen atom at the 1-position and the carbon atom at the 3-position in pyrazoline moiety, according to the fluorescence analysis. The fluorescence spectra of compound **3b** for detecting Cu^{2+} were studied. It was found that the compound **3b** exhibited Cu^{2+} -selective and sensitive chromogenic signaling behavior over other common physiologically important metal ions. The association constant K_a measured for coordination of sensor **3b** with Cu^{2+} was $4.56 \times 10^4 \text{ M}^{-1}$, and the detection limit of the sensor **3b** toward Cu^{2+} was $2.46 \times 10^{-8} \text{ M}$.

Materials and methods

Analytical procedure

A $1.0 \times 10^{-3} \text{ M}$ of stock solution of compound **3b** was prepared in DMF. The cationic stocks were all in H_2O with a concentration of 10^{-1} M for UV–vis absorption and fluorescence spectra analysis. For all measurements of fluorescence spectra, excitation was at 377 nm with 10.5 nm of excitation slit width and scan speed was set at 600 nm min^{-1} . UV–vis and fluorescence titration experiments were performed using $5 \times 10^{-5} \text{ M}$ and $1 \times 10^{-5} \text{ M}$ of compound **3b** in the DMF: H_2O = 1:1, respectively. For Cu^{2+} ion absorption and fluorescence titration experiments, 3 mL solution of compound **3b** ($5 \times 10^{-5} \text{ M}$) were filled in the quartz cell of 1 cm optical path length, and each time 1.5 μL solution of Cu^{2+} (10^{-2} M) and 1.0 μL solution of Cu^{2+} ($3 \times 10^{-3} \text{ M}$) were added into the quartz cell gradually by using a micro-syringe, respectively. After each addition of Cu^{2+} ion, the solution was stirred for 3 min. The volume of cationic stock solution added was less than 100 μL with the purpose of keeping the total volume of testing solution without obvious change.

Oscillator strength and quantum yields

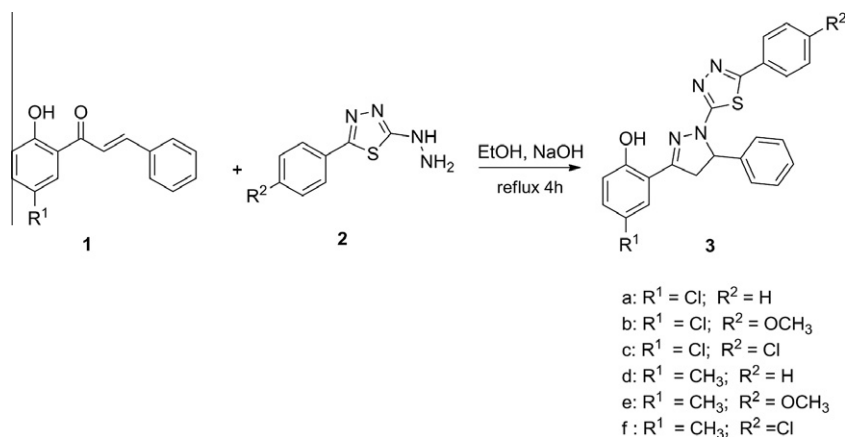
The Stokes shift ($\Delta\nu$) and oscillator strength (f) are important characteristics for the fluorescent compounds [41]. The Stokes shift is a parameter that indicates differences in the properties and structure of the fluorophores between the ground state S_0 and the first excited state S_1 . The Stokes shift (cm^{-1}) was calculated by the following equation:

$$(V_A - V_F) = (1/V_A - 1/V_F) \times 10^7 \quad (1)$$

The oscillator strength (f) shows the effective number of electrons whose transition from ground to excited state gives the absorption area in the electron spectrum. The oscillator strength was calculated by Eq. (2). The ϵ_{max} is molar extinction coefficient and $\Delta\nu_{1/2}$ is the width of the absorption band (cm^{-1}) at 1/2 (ϵ_{max}).

$$f = 4.32 \times 10^{-9} \Delta\nu_{1/2} \epsilon_{\text{max}} \quad (2)$$

The ability for the molecules to emit the absorbed light energy is characterized quantitatively by the fluorescence quantum yield (Φ_F). Quantum yield was determined by the relative comparison procedure, using quinine sulfate dehydrate ($\geq 99.0\%$) in 0.1 N H_2SO_4 as the main standard. The corrected emission spectra were measured for the quinine sulfate dehydrate standard ($\lambda_{\text{ex}} = 380 \text{ nm}$; $A(\text{Absorption}) < 0.01$; $\Phi_F = 0.510$) [42]. For all the measurements of



Scheme 1. Synthesis of 1,3,5-triaryl pyrazoline derivatives.

fluorescence spectra, scan speed was 600 nm min⁻¹ using a quartz cell of 1 cm optical path length. And the UV–vis absorption spectra were recorded in a standard 1 cm path length quartz cell in range 250–600 nm with spectral resolution 1 nm. The general equation used in the determination of relative quantum yields from earlier research was given in Eq. (3) [21].

$$\Phi_F = (\Phi_{FS})(FAu)(A_s)(\eta_u^2)/(FAS)(Au)(\eta_s^2) \quad (3)$$

where Φ_F and F_A are fluorescence quantum yield and integrated area under the corrected emission spectrum, respectively; A is absorbance at the excitation wavelength; η represent the refractive index of the solution; and the subscripts u and s refer to the unknown and the standard, respectively. Furthermore, the energy yield off fluorescence (E_F), which is calculated by Eq. (4), also can be used instead of the fluorescence quantum yield (Φ_F).

$$E_F = \Phi_F(\lambda A/\lambda F) \quad (4)$$

General procedure for the synthesis of compounds **3a–f**

To a stirred solution of substituted chalcone (**1**) (1.0 mmol) in ethanol (15 mL) was added 5-aryl-2-hydrazinyl-1,3,4-thiadiazole (**2**) (1.2 mmol) and NaOH (3.0 mmol) and the reaction mixture was refluxed for 3–6 h as shown in Scheme 1. The progress of the reaction was monitored by TLC. The reaction mixture was allowed to cool to room temperature, and the solvent was evaporated under reduced pressure. The residue was dissolved in dichloromethane (30 mL), and then washed with water (50 mL) and brine (20 mL). The organic layer was collected and dried over MgSO₄. After filtration, the solvent was removed under reduced pressure. The crude product was purified by silica gel column chromatography with petroleum dichloromethane/ethyl acetate (15:1; v/v) as the eluting solvent to give the desired products **3a–3f**.

The spectroscopic data of compounds **3a–3f**

4-Chloro-2-(5-phenyl-1-(5-phenyl-1,3,4-thiadiazol-2-yl)-4,5-dihydro-1H-pyrazol-3-yl)phenol (3a). Yellow solid, yield 67.4%; mp 228–230 °C; IR (KBr, cm⁻¹): 3192.6, 3063.1, 3026.4, 2921.7, 1614.3, 1587.9, 1522.5, 1483.0; ¹H NMR (400 MHz, CDCl₃): δ 3.48 (dd, 1H, $J = 6.6, 17.6$ Hz, 4-H_{trans}), 4.05 (dd, 1H, $J = 12.0, 17.6$ Hz, 4-H_{cis}), 5.72 (dd, 1H, $J = 6.6, 12.0$ Hz, 5-H of pyrazoline), 7.04 (d, 1H, $J = 8.9$ Hz, Ar–H), 7.18 (d, 1H, $J = 2.7$ Hz, Ar–H), 7.31–7.48 (m, 9H, Ar–H), 7.80–7.82 (m, 2H, Ar–H), 9.89 (s, 1H, OH); HRMS: calcd for [M+H]⁺ C₂₃H₁₇ClN₄O₂S: 433.0890; found: 433.0913.

4-Chloro-2-(1-(5-(4-methoxyphenyl)-1,3,4-thiadiazol-2-yl)-5-phenyl-4,5-dihydro-1H-pyrazol-3-yl)phenol (3b). Yellow solid, yield 80.3%; mp 241–243 °C; IR (KBr, cm⁻¹): 3242.2, 3058.2, 3028.7, 2931.3, 1607.7, 1574.9, 1524.7, 1458.9; ¹H NMR (300 MHz, CDCl₃): δ 3.46 (dd, 1H, $J = 6.3, 17.7$ Hz, 4-H_{trans}), 3.84 (s, 3H, CH₃), 4.07 (dd, 1H, $J = 12.0, 17.7$ Hz, 4-H_{cis}), 5.76 (dd, 1H, $J = 6.3, 12.0$ Hz, 5-H of pyrazoline), 6.92 (d, 2H, $J = 9.6$ Hz, Ar–H), 7.02 (d, 1H, $J = 9.0$ Hz, Ar–H), 7.16 (d, 1H, $J = 2.4$ Hz, Ar–H), 7.27–7.40 (m, 6H, Ar–H), 7.73 (d, 2H, $J = 8.7$ Hz, Ar–H), 9.87 (s, 1H, OH); HRMS: calcd for [M+H]⁺ C₂₄H₁₉ClN₄O₂S: 463.0995; found: 463.0993.

4-Chloro-2-(1-(5-(4-chlorophenyl)-1,3,4-thiadiazol-2-yl)-5-phenyl-4,5-dihydro-1H-pyrazol-3-yl)phenol (3c). Yellow solid, yield 43.3%; mp 267–268 °C; IR (KBr, cm⁻¹): 3435.2, 3199.3, 3057.6, 3023.2, 2922.3, 1615.1, 1588.1, 1519.9, 1483.4; ¹H NMR (300 MHz, CDCl₃): δ 3.48 (dd, 1H, $J = 6.0, 18.0$ Hz, 4-H_{trans}), 4.11 (dd, 1H, $J = 12.0, 18.0$ Hz, 4-H_{cis}), 5.82 (dd, 1H, $J = 6.0, 12.0$ Hz, 5-H of pyrazoline), 7.01 (d, 1H, $J = 9.0$ Hz, Ar–H), 7.16 (d, 1H, $J = 2.4$ Hz, Ar–H), 7.27–7.39 (m, 8H, Ar–H), 7.70 (d, 2H, $J = 8.1$ Hz, Ar–H), 9.78 (s, 1H, OH); HRMS: calcd for [M+H]⁺ C₂₃H₁₆Cl₂N₄O₂S: 467.0500; found: 467.0512.

4-Methyl-2-(5-phenyl-1-(5-phenyl-1,3,4-thiadiazol-2-yl)-4,5-dihydro-1H-pyrazol-3-yl)phenol (3d). Yellow solid, yield 63.9%; mp 236–238 °C; IR (KBr, cm⁻¹): 3166.4, 3063.1, 3027.2, 2920.1, 1622.3, 1594.3, 1525.2, 1493.6; ¹H NMR (300 MHz, CDCl₃): δ 2.28 (s, 3H, CH₃), 3.52 (dd, 1H, $J = 6.0, 17.7$ Hz, 4-H_{trans}), 4.12 (dd, 1H, $J = 11.1, 17.7$ Hz, 4-H_{cis}), 5.84 (dd, 1H, $J = 6.0, 11.1$ Hz, 5-H of pyrazoline), 6.99 (d, 2H, $J = 8.4$ Hz, Ar–H), 7.17 (dd, 1H, $J = 1.5, 8.4$ Hz, Ar–H), 7.30–7.42 (m, 8H, Ar–H), 8.05 (dd, 2H, $J = 3.0, 6.6$ Hz, Ar–H), 9.67 (s, 1H, OH); HRMS: calcd for [M+H]⁺ C₂₄H₂₀N₄O₂S: 413.1436; found: 413.1461.

2-(1-(5-(4-Methoxyphenyl)-1,3,4-thiadiazol-2-yl)-5-phenyl-4,5-dihydro-1H-pyrazol-3-yl)-4-methylphenol (3e). Yellow solid, yield 84.7%; mp 236–237 °C; IR (KBr, cm⁻¹): 3206.6, 3068.8, 3031.0, 2931.7, 2910.8, 1606.2, 1572.9, 1493.7, 1483.5; ¹H NMR (300 MHz, CDCl₃): 2.29 (s, 3H, CH₃), 3.50 (dd, 1H, $J = 6.0, 16.8$ Hz, 4-H_{trans}), 3.84 (s, 3H, CH₃), 4.10 (dd, 1H, $J = 13.2, 16.8$ Hz, 4-H_{cis}), 5.80 (dd, 1H, $J = 6.0, 13.2$ Hz, 5-H of pyrazoline), 6.93 (d, 2H, $J = 9.0$ Hz, Ar–H), 7.00 (d, 2H, $J = 8.4$ Hz, Ar–H), 7.17 (d, 1H, $J = 9.0$ Hz, Ar–H), 7.29–7.42 (m, 5H, Ar–H), 7.74 (d, 2H, $J = 8.7$ Hz, Ar–H), 9.68 (s, 1H, OH); HRMS: calcd for [M+H]⁺ C₂₅H₂₂N₄O₂S: 443.1542; found: 443.1522.

2-(1-(5-(4-Chlorophenyl)-1,3,4-thiadiazol-2-yl)-5-phenyl-4,5-dihydro-1H-pyrazol-3-yl)-4-methylphenol (3f). Yellow solid, yield 55.4%; mp 246–247 °C; IR (KBr, cm⁻¹): 3251.0, 3026.8, 2921.5, 1619.9, 1587.5, 1520.8, 1491.1; ¹H NMR (300 MHz, CDCl₃): 2.28 (s, 3H, CH₃), 3.51 (dd, 1H, $J = 5.4, 18.0$ Hz, 4-H_{trans}), 4.12 (dd, 1H, $J = 12.9, 18.0$ Hz, 4-H_{cis}), 5.80 (dd, 1H, $J = 5.4, 12.9$ Hz, 5-H of pyrazoline), 6.98 (d, 2H, $J = 8.4$ Hz, Ar–H), 7.17 (d, 1H, $J = 9.3$ Hz, Ar–H), 7.30–7.41 (m, 7H, Ar–H), 7.72 (d, 2H, $J = 8.4$ Hz, Ar–H), 9.63 (s, 1H, OH); HRMS: calcd for [M+H]⁺ C₂₄H₁₉ClN₄O₂S: 447.1046; found: 447.1071.

X-ray crystallography

Suitable single crystals of **3b** for X-ray structural analysis were obtained by slow evaporation of a solution of the solid in dichloromethane at room temperature for 14 days. The diffraction data were collected with a Bruker SMART CCD diffractometer using a graphite monochromated Mo K α radiation ($\lambda = 0.71073$ Å) at 298 K. The structures were solved by direct methods with SHELXS-97 program and refinements on F^2 were performed with SHELXL-97 program by full-matrix least-squares techniques with anisotropic thermal parameters for the non-hydrogen atoms. All H atoms were initially located in a difference Fourier map. The methyl H atoms were then constrained to an ideal geometry, with C–H = 0.96 Å and U_{iso}(H) = 1.5 Ueq(C). All other H atoms were placed in geometrically idealized positions and constrained to ride on their parent atoms, with C–H = 0.93 Å and U_{iso}(H) = 1.2 Ueq(C).

Results and discussion

Synthesis of compounds **3**

The synthetic routes of the proposed compounds **3** are outlined in Scheme 1. The chalcone derivatives (**1**) and 5-aryl-2-hydrazinyl-1,3,4-thiadiazole (**2**) were prepared according to the literature [43,44]. The 3,5-diarylpyrazoline derivatives **3a–f** were obtained by the reaction of chalcone **1** with 5-aryl-2-hydrazinyl-1,3,4-thiadiazole **2** under reflux condition in 43.3–84.7% yields. The structures of compounds (**3a–f**) were confirmed by IR, ¹H NMR and HRMS spectral data. The IR spectra of all the compounds **3a–f** showed ν (C=N) stretch at 1587–1607 cm⁻¹ consisting with pyrazoline and thiadiazole moiety. In the ¹H NMR spectra of compounds that is shown in Fig. 1, the CH₂ protons of the pyrazoline ring resonated as a pair of doublets at δ 3.46–3.52 ppm (H_A), 4.05–

4.12 ppm (H_B). The CH proton at C5 also appeared as a doublet of doublets at δ 5.72–5.84 ppm due to vicinal coupling with the two magnetically non-equivalent protons of the methylene. The hydroxy proton signal appeared at the range of δ = 9.63–9.89 ppm as a single peak. HRMS showed that found $[M+H]^+$ -ion peak accorded with calculated value. Moreover, typically, the structure of compound **3b** was confirmed by X-ray diffraction analysis.

X-ray crystallography

The spatial structure of compounds **3b** was determined by using X-ray diffraction analysis as shown in Fig. 2. A summary of crystallographic data collection parameters and refinement parameters for **3b** is compiled in Table S1. The structure of compound **3b** is crystallized in monoclinic space group $C2/c$. Two benzene moieties and a thiaziazole moiety are bonded to the pyrazoline ring at the atoms of C7, C9 and N2, respectively. In the crystal of **3b**, torsion angle $C(10)-C(9)-N(2)-C(16)$ of $-73.5(4)$, shows C10 in the thiaziazole moiety adopts an antiperiplanar conformation with respect to the C16 atom of the benzene ring. In the asymmetry unit, the thiaziazole ring, benzene rings and pyrazoline are almost coplanar. And the pyrazoline ring makes dihedral angles with benzene A and thiaziazole ring of $5.0(19)^\circ$ and $9.4(18)^\circ$, respectively, while the dihedral angle between pyrazoline and benzene A moiety is $82.5(2)^\circ$. The dihedral angle of benzene and thiaziazole is $6.8(18)^\circ$.

Regarding the crystal structure of **3b**, there is one intramolecular $C(23)-H(23)\cdots S$ hydrogen bond forming a pseudo five-membered ring. The molecules are connected by weak $\pi-\pi$ interactions and further assigned into layers via intramolecular hydrogen bond of $C(8)-H(8)\cdots Cl$, $H(8)\cdots Cl$, 2.79 \AA , $C(8)\cdots Cl$ $3.549(3) \text{ \AA}$, $C(8)-H(8)\cdots Cl$ 140° with the symmetry code of $1/2 - x, -1/2 + y, 3/2 - z$ along the b -axis (Fig. S1). Besides the aforementioned hydrogen bonds, there is also a weak $C-H\cdots\pi$ interaction, which is, however, important for the packing modes $C(15)\cdots Cg(2)$ $2.974(4)^\circ$.

Optical properties of compounds **3a-f**

UV-vis absorption spectra

The UV-vis absorption spectra of compounds **3a-f** shown in Fig. S2 and Table 1 have been recorded in dichloromethane solution with the concentration of $2.5 \times 10^{-5} \text{ M}$. As we all know, the pyrazoline derivative is chromophoric π -system composed of two aryl substituents in the 1- and 3-position and three out of the five pyrazoline ring atoms (N1–N2–C3). The remaining two carbon atoms (C4 and C5) of the ring are sp^3 hybridized and are not part of the conjugated p -system. Absorption spectra of each compound exhibit a strong, featureless absorption band, which can be assigned to an allowed

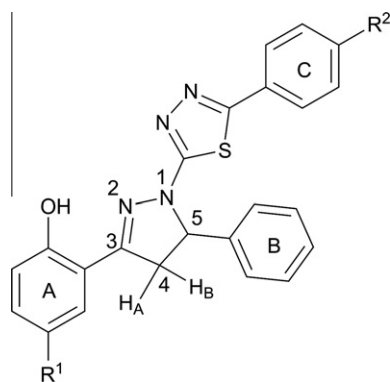


Fig. 1. Structure of compounds **3**.

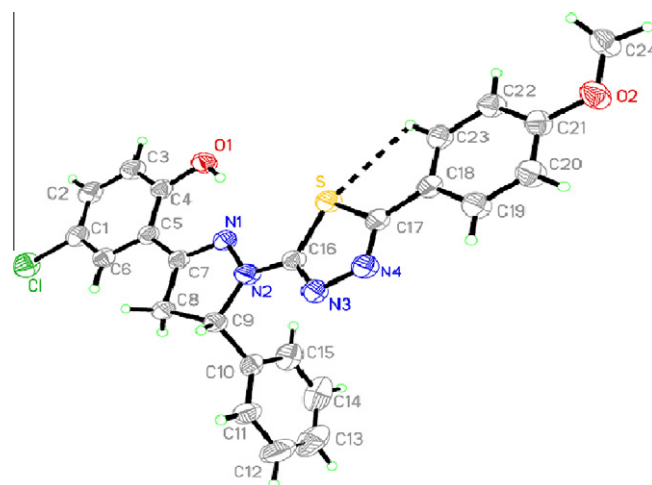


Fig. 2. Molecular structure of compound **3b** with displacement ellipsoids drawn at the 30% probability level.

$\pi-\pi^*$ transition of the conjugated backbone localized on the pyrazoline ring system [45]. It can be seen that the spectral shapes are very similar due to these compounds possess a similar structure. But a small definite substituent effect was observed such that electron-withdrawing groups (Cl) result in a red shift with respect to an electron-donating group (MeO). The data indicated that, when a chlorine group is located on the phenyl ring (C ring), the absorption peaks of **3c** and **3f** are at longer wavelengths than those of **3b** and **3e** in which the methoxyl group is bonded.

Our group has previously reported the synthesis of several pyrazoline or bis-pyrazoline derivatives containing pyridazine, thiazole or ferrocene moiety, which have good blue fluorescence [36,37,46,47]. But the maximum absorptions were fixed at 327, 342, and 347 nm, respectively, and except the bis-pyrazoline derivatives which the maximum absorption was fixed at 370 nm. Otherwise, the single-pyrazoline derivatives we reported in this paper have the minimum absorption at 366 nm and the maximum at 370 nm. The phenomenon are attributed to the incorporation of the 1,3,4-thiaziazole enhanced the conjugated structure of pyrazoline ring.

Effect of solvent on the absorption spectra

Typical absorption spectra of compound **3b** in different solvents were shown in Fig. S3 in Supplementary data, and the corresponding absorption wavelength maxima and molar extinction coefficient (ϵ) values were presented in Table 2. As shown in Table 2, absorption wavelength maxima and molar extinction coefficient values of compound **3b** in different solvents varied from 371 to 366 nm and from 2.46 to 2.90 ($10^4 \text{ M}^{-1} \text{ cm}^{-1}$), respectively. It was observed that the absorption spectra of these compounds change very little with increasing solvent polarity indicating that there is no charge transfer in the ground state [48].

Fluorescence spectra

Following the absorption experiments, steady-state fluorescence spectra of compounds **3a-f** were obtained in dichloromethane solution with concentration of $2.5 \times 10^{-6} \text{ M}$. As shown in Table 1 and Fig. 3 the maximal emission bands were all in the range of 431–457 nm. It can be observed that an electron-withdrawing group such as chlorine group in benzene ring (A ring) made the emission wavelength of **3a**, **3b** and **3c** red shifted than that of compounds **3d**, **3e** and **3f** with methyl group in the benzene ring. The relative shifts in the emission spectra were attributed to the nature of the electronic transition ($\pi-\pi^*$) involving an intramolecular charge transfer from the $Ar-N1$ donor to the $Ar^A-C3=N2$

Table 1
The optical characteristics of the compounds **3a–f** in dichloromethane solution.

Compounds	λ_{abs} (nm)	ε ($10^4 \text{ M}^{-1} \text{ cm}^{-1}$)	λ_{ex} (nm)	λ_{em} (nm)	$\Delta\nu$ (cm^{-1})	f	Φ_{F}	E_{F}
3a	368	2.75	373	443	4236	0.69	0.10	0.083
3b	368	2.90	376	457	4714	0.76	0.20	0.161
3c	370	2.92	376	439	3817	0.73	0.13	0.109
3d	368	2.69	369	431	3898	0.66	0.02	0.017
3e	366	2.74	374	442	4114	0.63	0.07	0.058
3f	370	2.94	376	432	3448	0.73	0.04	0.034

Table 2
The optical characteristics of the compound **3b** in different solvents.

Compound	λ_{abs} (nm)	ε ($10^4 \text{ M}^{-1} \text{ cm}^{-1}$)	λ_{ex} (nm)	λ_{em} (nm)	ν (cm^{-1})	f	Φ_{F}	E_{F}
DCM	368	2.90	376	457	4714	0.76	0.20	0.161
THF	369	2.77	377	457	4643	0.70	0.24	0.194
DMF	371	2.76	376	455	4618	0.72	0.27	0.220
Acetonitrile	367	2.75	363	459	5762	0.71	0.19	0.152
Toluene	366	2.46	377	455	4547	0.69	0.25	0.201

acceptor. Along with the charge transfer, increased charge densities were found for the atoms N2 and C3 of pyrazoline ring in the first excited state S1 [49]. With increasing electron-withdrawing capacity of the Ar^A, the lone pair electrons on N1 were more delocalized toward the 3-substituted phenyl ring, and hence the charge transfer character of the emission state increased. Furthermore, for given substituent Ar^A, electronic character of substituent Ar^C also affected the emission wavelength and intensity, as effective as the substituent Ar^A. For example, compounds **3b** and **3e** which possess substituent methoxy group in the phenyl ring (**C ring**) have red-shift phenomenon compared with **3c** and **3f** which possess substituent chlorine. Besides above-mentioned phenomenon, we also found that the substituent Ar^C and Ar^A affected the fluorescence quantum yields of compounds **3a–f**. As listed in Table 1, when Ar^C with *p*-methoxyl group, the fluorescence quantum yield was higher than that when Ar^C with *p*-chlorophenyl group. For example, the quantum yields of compound **3b** and **3c** were 0.20 and 0.13, respectively. In addition, when Ar^A is with *m*-chloro group, the fluorescence quantum yield was higher than that of Ar^A with *m*-CH₃ group.

Effect of solvent on the emission spectra

Fluorescence spectra of compound **3b** in various solvents with different polarity were recorded in Fig. 4 and Table 2. As depicted in Fig. 4, the emission maxima had a red-shift from 455 to 459 nm and the Stokes shifts varied from 4547 to 5762 cm⁻¹ with increasing the polarity of the solvent from toluene to acetonitrile. The results might be resulted from the difference in the dipole moment of compound **3b** in the excited state and the ground state (i.e. $u_e > -u_g$). The relaxed excited state would be energetically stabilized relative to the ground state with increasing the polarity of solvents and a significant red-shift of the fluorescence band was observed. The stronger the interaction of solute and solvent, the lower the energy of the excited state, and the larger the red-shift of the emission band and the corresponding Stokes shift [50].

Effect of the concentration on the emission spectra

The effect of the concentration of compound **3b** on the fluorescence emission intensity was also studied. As shown in Fig. 5 the fluorescence intensity of the compound **3b** in dichloromethane increased initially and then decreased with increasing the concentration. This phenomenon was attributed to that the increase of molecule number of the compound **3b** with the increase of the concentration initially resulted in the increase of fluorescence intensity. However, when the concentration increased over to

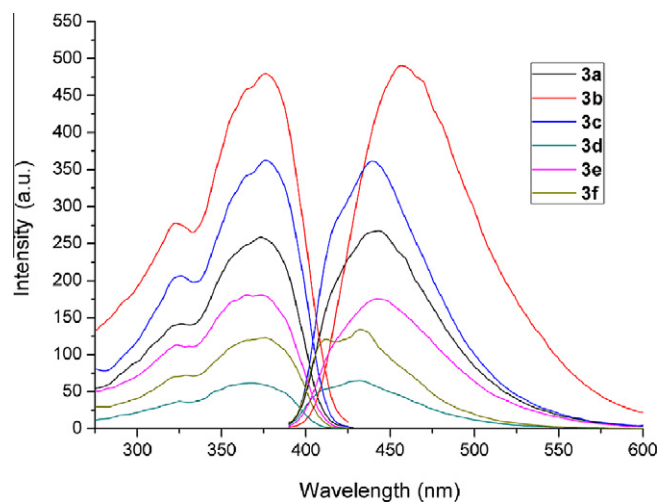


Fig. 3. Fluorescence excitation and emission spectra of compounds **3a–g** in dichloromethane solution with the concentration of 2.5×10^{-6} M. (The excitation and emission slit widths were 10 and 2.5 nm under normal light source, respectively.)

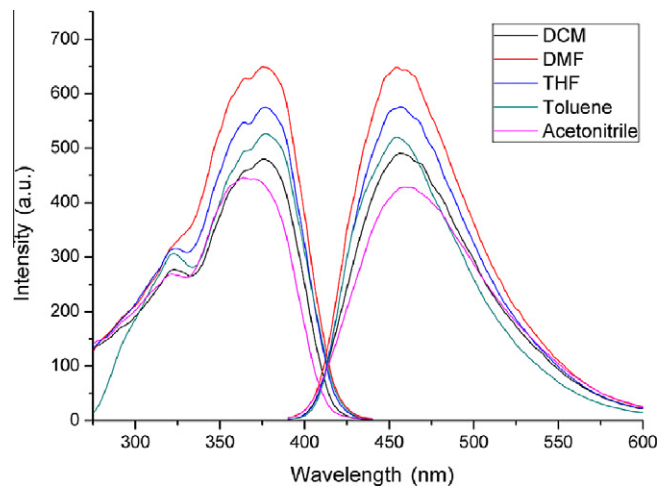


Fig. 4. Fluorescence excitation and emission spectra of compound **3b** in different solvents with the concentration of 2.5×10^{-6} M. (The excitation and emission slit widths were 10 and 2.5 nm under normal light source, respectively.)

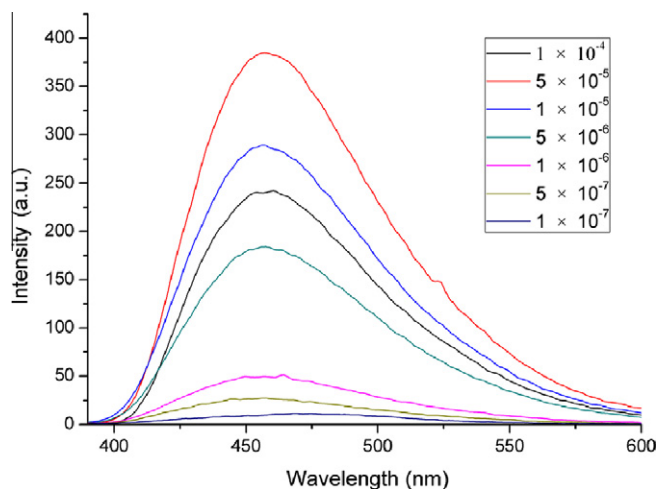


Fig. 5. Fluorescence emission spectra of compound **3b** in dichloromethane solution with different concentrations varied from 10^{-4} to 10^{-7} M. (The excitation and emission slit widths were 10 and 10 nm under 1% attenuation, respectively.)

5×10^{-5} M, the collision of fluorescent molecules with each other took place to quench the fluorescence [15]. In addition, maximum emission spectra of the compound **3b** in dichloromethane solution with varied concentrations were unchanged, which means that the fluorescent molecule structure was not changed, and kept single molecule in solution with increasing concentration, instead of di-aggregates, tri-aggregates or poly-aggregates molecule.

Fluorescent sensor for Cu^{2+}

UV–vis selectivity for Cu^{2+} studies

The optical response of the product **3b** to various metal ions was investigated by the UV–visible and emission spectroscopy. It is found that the compound **3b** can be used to determine Cu^{2+} ion with high selectivity and a low detection limit in the DMF:H₂O = 1:1 (v/v) solution. The absorption spectrum of compound **3b** exhibits a broad band at 375 nm at room temperature in the DMF:H₂O (1:1, v/v). Binding affinities of compound **3b** toward metal ions, Ag^+ , Al^{3+} , Ba^{2+} , Ca^{2+} , Cd^{2+} , Co^{2+} , Cr^{3+} , Cu^{2+} , Fe^{3+} , Hg^{2+} , K^+ , Mg^{2+} , Na^+ , Ni^{2+} , Pb^{2+} and Zn^{2+} ions were evaluated by UV–vis spectroscopy measurements. As shown in Fig. S4 upon interaction with metal ions, significant changes in absorption spectra were observed particularly with Cu^{2+} , the addition of Cu^{2+} caused a decrease of absorption intensity to some extent at 375 nm, and a new absorption peak appeared obviously at 390–410 nm. Other metal ions caused relatively minor changes in the absorption spectra of **3b**.

UV–vis absorption spectra titration studies

To investigate the binding property of compound **3b** toward Cu^{2+} , we measured the UV–vis absorption spectra of compound **3b** (1×10^{-5} M) in the presence of various concentrations of Cu^{2+} ion (0 – 3×10^{-5} M), as shown in Fig. 6. The absorbance of compound **3b** at 368 nm gradually decreases with an increasing concentration of Cu^{2+} ion. Moreover, two isobestic points at 330 nm and 390 nm were observed and a new absorption peak appears at the range of 390–410 nm, and its absorption intensity gradually increases with the addition of Cu^{2+} ion. This absorption peak is likely due to the coordination of compound **3b** with Cu^{2+} ion. Under comparable experimental conditions, the UV–vis spectrum of Cu^{2+} displayed no appreciable absorption between 220 and 600 nm within the appropriate concentration range. There is a linear dependence of the ratio of absorbance at 400 nm and absorbance at 368 nm as a

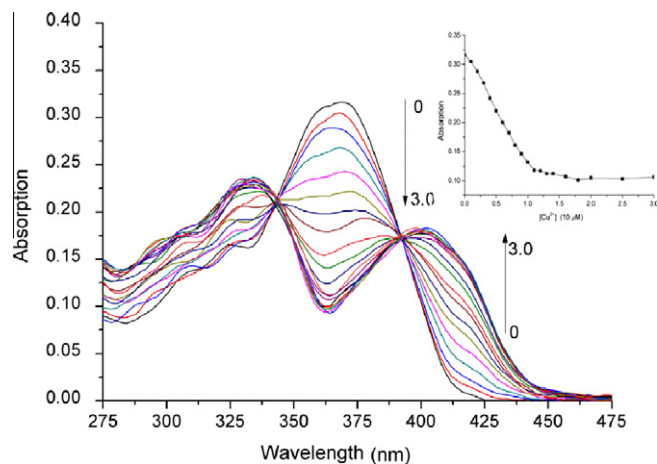


Fig. 6. Absorption spectra of **3b** ($10 \mu\text{M}$) upon the addition of Cu^{2+} (0 – 3.0 equiv.) in DMF:H₂O (1:1, v/v). Inset: Absorption changes of compound **3b** at 368 nm upon the addition of Cu^{2+} (0 – 3.0×10^{-5} M).

function of Cu^{2+} concentration (Fig. S5). The sensor can be used as a ratiometric sensor for detecting Cu^{2+} . According to the above phenomena, we can observe the transformation from free compound **3b** to the Cu^{2+} -coordinated species. The coordination stoichiometry between **3b** and Cu^{2+} ion was estimated to be 1:1 by a nonlinear curve fitting of the UV–vis titration results (inset) similar to Job's plot as depicted in Fig. S6.

Fluorescent selectivity for Cu^{2+}

To obtain an excellent chemosensor, high selectivity is essential. Herein, the fluorescence spectra of **3b** with various metal ions were conducted to examine the selectivity. As indicated in Fig. S7 there was no response to other metal ions except Cu^{2+} ions. Similarly, achieving a high selectivity for the analyte of interest over a complex background of potentially competing species is a challenge in the development of sensors. Thus, the competition experiments were also conducted in the presence of 5.0 equiv. Cu^{2+} ion mixed with 50.0 equiv. other cations. As shown in Fig. S8 only Cr^{3+} , Fe^{3+} and Al^{3+} slightly disturbed the intensity by comparison with that without the other metal ions besides Cu^{2+} . Therefore, these results

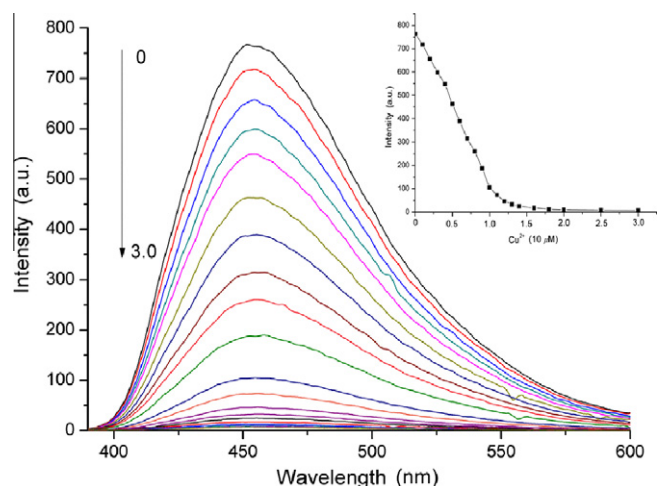


Fig. 7. Fluorescence emission spectra of **3b** ($10 \mu\text{M}$) in DMF:H₂O (1:1, v/v) upon the addition of Cu^{2+} (0 – 3.0 equiv.). Excitation wavelength was 377 nm. Inset: variations of fluorescence intensity of compound **3b** (10^{-5} M) at 454 nm vs. equivalents of $[\text{Cu}^{2+}]$.

suggest that **3b** has a high fluorescent selectivity for Cu²⁺ in the presence of these tested foreign metal ions.

The fluorescence spectra of **3b** in different ratios of DMF/H₂O solution were studied. As shown in Fig. S9, we can arrive the conclusion that when the percent of DMF from 40 to 80, the compound **3** can well response to Cu²⁺. Considering the practicability, the DMF/H₂O (v/v = 1:1) is selected for further experiments.

Fluorescence titration studies

To illustrate the sensitivity of **3b** for Cu²⁺ ion fluorescence titration experiment was carried out by increasing the concentration of Cu²⁺ ion to the solution of **3b** in DMF/H₂O (v/v = 1:1) at room temperature. As shown in Fig. 7, as Cu²⁺ ion was gradually titrated, the fluorescence intensity of compound **3b** gradually reduced, and when the amount of Cu²⁺ ion added was about 1 equiv. (10 μM), the fluorescence intensity almost reached minimum. When more Cu²⁺ was titrated, the fluorescence intensity showed negligible changes. The nonlinear curve fitting of the fluorescence titration (inset) also gives a 1:1 stoichiometric ratio between compound **3b** and Cu²⁺ which consist with one by UV-vis spectra as shown in Fig. 6. The association constant (K_a) between compound **3b** and Cu²⁺ ion in the DMF:H₂O (1:1, v/v) was calculated to be $4.56 \times 10^4 \text{ M}^{-1}$ according to the literature [51] (Fig. S10).

Effect of pH on the fluorescence

The pH value of the environment around the fluorescent probe for metal ions usually shows somewhat of an effect on its performance because of the protonation or deprotonation reaction for the fluorophore or the hydrolysis reaction for the metal ions in the alkaline condition. The effects of pH on the fluorescence response of the new probe **3b** to Cu²⁺ were therefore investigated as shown in Fig. S11. We found that in a solution of DMF/water (1:1) the suitable pH span for Cu²⁺ determination is between pH 4–10. In this region, the free **3b** has no response, while addition of Cu²⁺ ion can lead to a remarkable response. The facts suggest efficient complexation between probe and Cu²⁺ ion. As a result, our Cu²⁺-selective receptors would be an ideal colorimetric chemosensor for monitoring Cu²⁺ in aqueous solution in the pH range of 4–10.

Quantitative studies

The quantitative response of compound **3b** toward Cu²⁺ ion was studied by the fluorescence titration and the linear calibration plots as shown in Fig. S12. The dynamic range for the determination of Cu²⁺ was determined to be linear up to 0–10 μM with correlation coefficient (R²) of 0.995 [52]. The limit of detection (LOD) is evaluated using $3\sigma_{bi}/m$ [53], where σ_{bi} is the standard deviation of the blank signals and m is the slope of the linear calibration plot. The LOD for determination of Cu²⁺ was thus calculated to be $2.46 \times 10^{-8} \text{ M}$.

Conclusions

In summary, a series of novel pyrazoline derivatives were designed and synthesized in 43.3–84.7% yields. The structures of the compounds were determined by IR, ¹H NMR, HRMS spectra. Representatively, the spatial structure of the compound **3b** was determined using X-ray diffraction analysis. The absorption maxima of the compounds vary from 366 to 370 nm depending on the group bound to benzene rings. The maximum emission spectra and the fluorescence quantum yield of the compounds in dichloromethane are dependent on group in benzene ring. The intensity of absorption and fluorescence was also correlated with substituents on two aryl rings. The absorption spectra of these compounds change very little with increasing solvent polarity. In addition, when the concentra-

tion of the compound **3b** increased over to $5 \times 10^{-5} \text{ M}$, the fluorescence quenching could be attributed to the collision of fluorescent molecules with each other. The compound **3b** was used for the determination of Cu²⁺ ion with high selectivity and a low detection limit in DMF:H₂O = 1:1 (v/v). This sensor formed a 1:1 complex with Cu²⁺ and showed a fluorescent quench with good tolerance of other metal ions. Moreover, this sensor is very sensitive with fluorometric detection limit of $2.46 \times 10^{-8} \text{ M}$.

Acknowledgment

This study was supported by 973 Program (2010CB933504).

Appendix A. Supplementary material

Supplementary data associated with this article can be found, in the online version, at <http://dx.doi.org/10.1016/j.saa.2012.12.062>.

References

- [1] Z.N. Siddiqui, T.N.M. Musthafa, A. Ahmad, A.U. Khan, *Bioorg. Med. Chem. Lett.* 21 (2011) 2860–2865.
- [2] F. Hayat, A. Salahuddin, S. Umar, A. Azam, *Eur. J. Med. Chem.* 45 (2010) 4669–4675.
- [3] P.C. Lv, D.D. Li, Q.S. Li, X. Lu, Z.P. Xiao, H.L. Zhu, *Bioorg. Med. Chem. Lett.* 21 (2011) 5374–5377.
- [4] Z.A. Kaplancikli, A. Özdemir, G. Turan-Zitouni, M.D. Altıntop, Ö.D. Can, *Eur. J. Med. Chem.* 45 (2010) 4383–4387.
- [5] H. Khalilullah, S. Khan, M.J. Ahsan, B. Ahmed, *Bioorg. Med. Chem. Lett.* 21 (2011) 7251–7254.
- [6] K. Manna, Y.K. Agrawal, *Eur. J. Med. Chem.* 45 (2010) 3831–3839.
- [7] N.D. Amnerkar, K.P. Bhusari, *Eur. J. Med. Chem.* 45 (2010) 149–159.
- [8] S. Bano, K. Javed, S. Ahmad, I.G. Rathish, S. Singh, M.S. Alam, *Eur. J. Med. Chem.* 46 (2011) 5763–5768.
- [9] Z.L. Gong, B.X. Zhao, W.Y. Liu, H.S. Lv, J. Photochem. Photobiol., A 218 (2011) 6–10.
- [10] Z.L. Gong, F. Ge, B.X. Zhao, *Sens. Actuators, B* 159 (2011) 148–153.
- [11] H.B. Shi, S.J. Ji, B. Bian, *Dyes Pigments* 73 (2007) 394–396.
- [12] J.L. Bricks, A. Kovalchuk, C. Trieflinger, M. Nofz, M. Büschel, A.I. Tolmachev, J. Daub, K. Rurack, *J. Am. Chem. Soc.* 127 (2005) 13522–13529.
- [13] X.H. Zhang, W.Y. Lai, T.C. Wong, Z.Q. Gao, Y.C. Jiang, S.K. Wu, H.L. Kwong, S.T. Lee, *Synth. Met.* 114 (2000) 115–117.
- [14] X.C. Gao, H. Cao, L.Q. Zhang, B.W. Zhang, Y. Cao, C.H. Huang, *J. Mater. Chem.* 9 (1999) 1077–1080.
- [15] G. Bai, J.F. Li, D.X. Li, C. Dong, X.Y. Han, P.H. Lin, *Dyes Pigments* 75 (2007) 93–98.
- [16] G. Chen, H.Y. Wang, Y. Liu, X.P. Xu, S.J. Ji, *Dyes Pigments* 85 (2010) 194–200.
- [17] Y.F. Sun, S.H. Xu, R.T. Wu, Z.Y. Wang, Z.B. Zheng, J.K. Li, Y.P. Cui, *Dyes Pigments* 87 (2010) 109–118.
- [18] K.M. Vyas, R.N. Jadeja, V.K. Gupta, K.R. Surati, *J. Mol. Struct.* 990 (2011) 110–120.
- [19] K.R. Surati, *Spectrochim. Acta Part A Mol. Biomol. Spectrosc.* 79 (2011) 272–277.
- [20] H. Huang, Y. Yu, Z.T. Gao, Y. Zhang, C.J. Li, X. Xu, H. Jin, W.Z. Yan, R.Q. Ma, J. Zhu, X. Shen, H.L. Jiang, L.L. Chen, J. Li, *J. Med. Chem.* 55 (2012) 7037–7053.
- [21] S.M. Song, D. Ju, J.F. Li, D.X. Li, Y.L. Wei, C. Dong, P.H. Lin, S.M. Shuang, *Talanta* 77 (2009) 1707–1714.
- [22] Y.F. Sun, Y.P. Cui, *Dyes Pigments* 81 (2009) 27–34.
- [23] Q. Liu, L. Gao, L. Wang, Z. Xie, D. Li, *Spectrosc. Spect. Anal.* 29 (2009) 2810–2814.
- [24] K.R. Suratia, B.T. Thaker, *Spectrochim. Acta Part A Mol. Biomol. Spectrosc.* 75 (2010) 235–242.
- [25] W. Kuzniak, J. Ebothe, I.V. Kityk, K.J. Plucinski, E. Gondekd, P. Szlachcice, T. Uchaczf, P. Armatysg, *Spectrochim. Acta Part A Mol. Biomol. Spectrosc.* 77 (2010) 130–134.
- [26] Q. Peng, X.H. Tang, *Chin. Chem. Lett.* 20 (2009) 13–16.
- [27] J.F. Li, D.X. Li, Y.Y. Han, S.M. Shuang, C. Dong, *Spectrochim. Acta Part A Mol. Biomol. Spectrosc.* 73 (2009) 221–225.
- [28] C.J. Fahrni, L.C. Yang, D.G. VanDerveer, *J. Am. Chem. Soc.* 125 (2003) 3799–3812.
- [29] A. Ciupa, M.F. Mahon, P.A.D. Bank, L. Caggiano, *Org. Biomol. Chem.* 10 (2012) 8753–8757.
- [30] A.P. Silva, H.Q.N. Gunaratne, T. Gunnlaugsson, A.J.M. Huxley, C.P. McCoy, J.T. Rademacher, T.E. Rice, *Chem. Rev.* 197 (1997) 1515–1566.
- [31] H. Tapiero, D.M. Townsend, K.D. Tew, *Copper Biomed. Pharmac.* 57 (2003) 386–398.
- [32] R.A. Lovstad, *Biomaterials* 17 (2004) 111–113.
- [33] M.Y. Pamukoglu, F. Kargi, *J. Hazard. Mater.* 148 (2007) 274–280.
- [34] P.G. Welsha, J. Liptona, C.A. Mebaneb, J.C.A. Marra, *Ecotoxicol. Environ. Saf.* 69 (2008) 199–208.

- [35] P. Kumar, R.K. Tewari, P.N. Sharma, *Plant Cell Rep.* 27 (2008) 399–409.
- [36] Z.L. Gong, L.W. Zheng, B.X. Zhao, D.Z. Yang, H.S. Lv, W.Y. Liu, S. Lian, *J. Photochem. Photobiol., A* 209 (2010) 49–55.
- [37] W.Y. Liu, Y.S. Xie, B.X. Zhao, B.S. Wang, H.S. Lv, Z.L. Gong, S. Lian, L.W. Zheng, *J. Photochem. Photobiol., A* 214 (2010) 135–144.
- [38] W.Y. Liu, H.Y. Li, H.S. Lv, B.X. Zhao, J.Y. Miao, *Spectrochim. Acta Part A Mol. Biomol. Spectrosc.* 95 (2012) 658–663.
- [39] W.Y. Liu, H.Y. Li, B.X. Zhao, J.Y. Miao, *Org. Biomol. Chem.* 9 (2011) 4802–4805.
- [40] W.Y. Liu, H.Y. Li, B.X. Zhao, J.Y. Miao, *Analyst* 137 (2012) 3466–3469.
- [41] H. Shakia, K. Gharanjiga, S. Rouhania, A. Khosravi, *J. Photochem. Photobiol., A* 216 (2010) 44–50.
- [42] R.A. Velapoldi, K.D. Mielenz, *A Fluorescence Standard Reference Material: Quinine Sulfate Dihydrate*. National Bureau of Standards (Now, The National Institute of Standards and Technology, NIST) Special Publication, Washington DC, US, 1980, pp. 260–264.
- [43] A. Budakoti, A.R. Bhat, A. Azam, *Eur. J. Med. Chem.* 44 (2009) 1317–1325.
- [44] S.A. Carvalho, E.F. Silva, R.M. Santa-Rita, S.L. Castrod, C.A.M. Fraga, *Bioorg. Med. Chem. Lett.* 14 (2004) 5967–5970.
- [45] C.J. Fahrni, L. Yang, D.G. VanDerveer, *J. Am. Chem. Soc.* 125 (2003) 3799–3812.
- [46] Z.L. Gong, Y.S. Xie, B.X. Zhao, H.S. Lv, W.Y. Liu, L.W. Zheng, S. Lian, *J. Fluoresc.* 21 (2011) 355–364.
- [47] Z.L. Gong, L.W. Zheng, B.X. Zhao, *J. Lumin.* 132 (2012) 318–324.
- [48] J.F. Li, B. Guan, D.X. Li, C. Dong, *Spectrochim. Acta Part A Mol. Biomol. Spectrosc.* 68 (2007) 404–408.
- [49] K. Rurack, J.L. Bricks, B. Schulz, M. Maus, G. Reck, U. Resch-Genger, *J. Phys. Chem. A* 104 (2000) 6171–6188.
- [50] C. Reichardt, *Solvents and solvent effects in organic chemistry*, third ed., Wiley-VCH, Marburg, 2004, pp. 352–353.
- [51] M.J. Yuan, W.D. Zhou, X.F. Liu, M. Zhu, J.B. Li, X.D. Yin, H.Y. Zheng, Z.C. Zuo, C.B. Ouyang, H.B. Liu, Y.L. Li, D.B. Zhu, *J. Org. Chem.* 73 (2008) 5008–5014.
- [52] N. Li, Y. Xiang, X.T. Chen, A.J. Tong, *Talanta* 79 (2009) 327–332.
- [53] B.P. Joshi, J. Park, W.I. Lee, K.H. Lee, *Talanta* 78 (2009) 903–909.